

13.1

## Effect of Growth Temperature on the Physicochemical Properties of Low-Temperature GaAs Layers Fabricated by Pulsed Laser Deposition

© R.N. Kriukov, Yu.A. Danilov, V.P. Lesnikov, O.V. Vikhrova, S.Yu. Zubkov

Lobachevsky State University, Nizhny Novgorod, Russia  
E-mail: kriukov.ruslan@yandex.ru

Received September 21, 2022

Revised December 12, 2022

Accepted December 12, 2022

Low-temperature device-quality GaAs layers with high resistivity were obtained by pulsed laser deposition. The properties of GaAs layers are sensitive to the process temperature. At a growth temperature of less than 300°C, the layers have low electron mobility and a shift of the GaAs stoichiometry towards the region of arsenic enrichment at a level of 1–2 at.%. At a growth temperature of more than 300°C, the layers show an improved crystalline quality. The dependence of the relative intensity of the As 3d photoelectron line on the growth temperature confirms this trend with a change in the growth temperature.

**Keywords:** pulsed laser deposition, Hall effect, X-ray photoelectron spectroscopy.

DOI: 10.21883/TPL.2023.02.55370.19372

The first reports on growth of GaAs layers at a low temperature (LT-GaAs) have been published in the 1980s [1]. LT-GaAs is formed almost exclusively by molecular beam epitaxy (MBE) with an excess supply of arsenic into the growth chamber [2]. The short lifetime of nonequilibrium carriers and high resistivity values are regarded as consequent effects of the As excess in grown layers [3]. These properties are key to several important applications of LT-GaAs (specifically, its use in generators and detectors of terahertz radiation [4] and ultrafast photoreceivers [5]). These layers are also used in technological processes as, e.g., dislocation filters for growth of GaAs/Si heterostructures [6] and cover layers for structures with quantum dots [7].

A few studies focused on LT-GaAs synthesized by metalorganic vapor phase epitaxy have already been published [8,9]. However, this method can only loosely be classified as a low-temperature GaAs growth technique, since the growth rate decreases markedly at lower substrate temperatures ( $T_s$ ): specifically, it drops to 0.05 nm/s at 445°C and to zero at 400°C [8]) due to a reduction in the rate of trimethylgallium decomposition. In addition, the concentration of uncontrolled acceptors (carbon) in layers increases with decreasing  $T_s$  [8]. The method of pulsed laser deposition (PLD) in vacuum is free from these drawbacks: the rate of deposition of the sputtered material in this process depends only marginally on  $T_s$ . Although the PLD method is used successfully to form ferromagnetic GaAs layers doped heavily with transition elements (Fe) [10], the properties of undoped gallium arsenide synthesized this way have not been examined yet.

A proprietary setup (cylindrical stainless-steel vacuum chamber with a quartz window for laser radiation input) was used to grow LT-GaAs layers. The base pressure in the chamber was  $7 \cdot 10^{-5} - 10^{-4}$  Pa. The distance between

a rotating target and a substrate was approximately equal to 8 cm. Undoped GaAs served as the target. Pulsed second-harmonic radiation (wavelength: 532 nm; pulse energy:  $\sim 250$  mJ; pulse duration: 10 ns) of an LQ-529 Nd:YAG laser was focused into a spot  $\sim 1.5$  mm<sup>2</sup> in size on the target. The pulse repetition frequency was 10 Hz. Semi-insulating GaAs(100) (epi-ready) substrates were treated with an HF:H<sub>2</sub>O=1:10 solution to remove natural oxide immediately prior to introduction into the growth chamber; before the growth procedure, they were also subjected to thermal treatment at 400°C for 30 min in the chamber. LT-GaAs layers were deposited within 25 min at  $T_s = 60 - 450$  °C at a growth rate of  $\sim 2$  nm/min.

The electric parameters of structures were measured using the Hall effect (Nanometrics HL5500 setup). XPS (X-ray photoelectron spectroscopy) studies of samples were performed using an Omicron Multiprobe RM system (Omicron Nanotechnology GmbH, Germany). The emission of photoelectrons was excited by MgK<sub>α</sub> radiation (1253.6 eV). Photoelectron lines O 1s, C 1s, As 3d, and Ga 3d were recorded in the experiment. The depth of analysis was  $3\lambda \sim 5$  nm. The value of  $\lambda$  (free path depth of a photoelectron) was calculated in accordance with the procedure outlined in [11]. The diameter of the analyzed region was 3 mm. A residual gas pressure of  $5 \cdot 10^{-7}$  Pa was maintained in the chamber. Layer-by-layer profiling was performed via etching by Ar<sup>+</sup> ions with an energy of 1 kV. The pressure in the chamber was maintained at  $4 \cdot 10^{-4}$  Pa in the process. The angle between the ion gun axis and the normal to the sample surface was 45°. The ion current measured at the sample during etching was 3.8 μA. At any stage of the experiment, the sample temperature did not exceed 50–60°C. Spectral analysis was performed in SDP v. 4.3 and CasaXPS in accordance with the spectra correction algorithm detailed in [12].

The surface of layers (see Fig. 1) was examined with a Solver Pro (NT-MDT, Russia) atomic force microscope (AFM). The root-mean-square (RMS) surface roughness after layer growth was 0.1–0.2 nm. The analysis of surface topography after ion etching revealed that the profiling regimes used did not induce any substantial surface modification.

It follows from the results of Hall measurements that sheet resistance  $R$  of the LT-GaAs/substrate structure decreases somewhat compared to  $R_s$  of the substrate without a grown layer ( $5.4 \cdot 10^9 \Omega/\text{sq}$ ). Both the substrate and LT-GaAs featured  $n$ -type conductivity. The LT-GaAs layer resistance ( $R_1$ ) was calculated using the bilayer model [13]:

$$R_1 = RR_s/(R_s - R),$$

$$\mu_1 = (\mu - \mu_s/(1 + \beta^{-1}))(1 + \beta) \text{ at } \beta = R_1/R_s,$$

where  $R_1$  is the layer resistance,  $R_s$  is the substrate resistance,  $R$  is the structure resistance measured using the Hall effect,  $\mu_1$  is the effective electron mobility in the layer,  $\mu$  is the measured mobility value, and  $\mu_s$  is the carrier mobility in the substrate ( $4810 \text{ cm}^2/(\text{V} \cdot \text{s})$ ). The results of calculations are presented in Fig. 2 for different growth temperatures. The resistivity of LT-GaAs ( $5 \cdot 10^3$ – $4 \cdot 10^4 \Omega \cdot \text{cm}$ ) is comparable to the values obtained in MBE [2].

The mobility of electrons in LT-GaAs layers grown at temperatures below  $250^\circ\text{C}$  was  $\sim 20 \text{ cm}^2/(\text{V} \cdot \text{s})$ . This parameter increases sharply at  $T_s = 300^\circ\text{C}$  and tends to the typical substrate value at higher temperatures (Fig. 2). The shape of the  $R_1(T_s)$  dependence (Fig. 2) implies that temperature  $T_s = 300^\circ\text{C}$  is the critical one. At higher growth temperatures, the electron mobility increases due

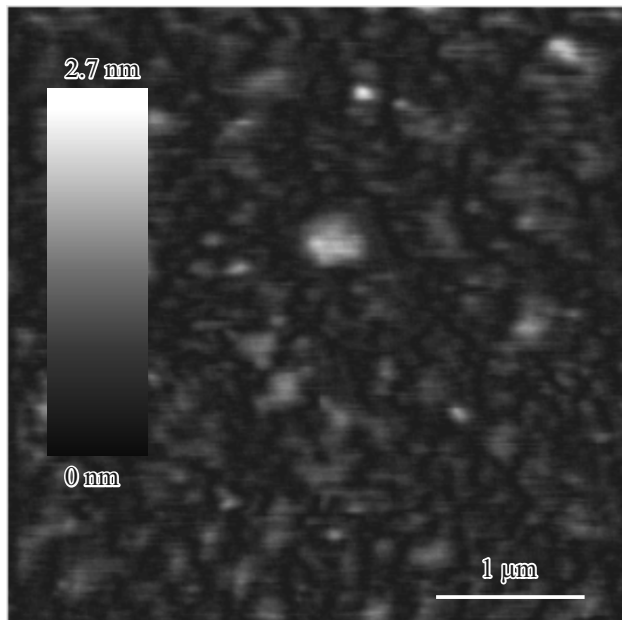


**Figure 1.** AFM image of the surface of an LT-GaAs layer grown at  $T_s = 150^\circ\text{C}$ .

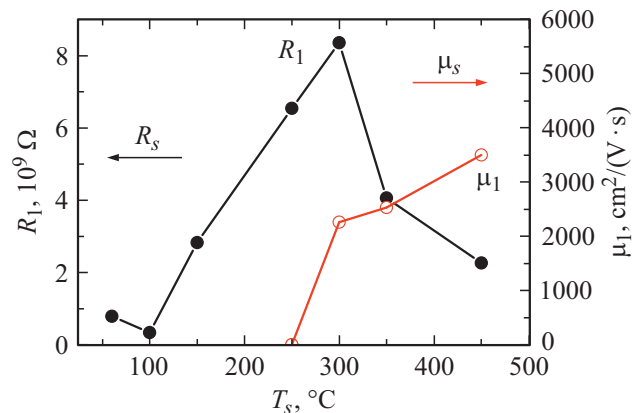


**Figure 2.** Dependences of resistance  $R_1$  and mobility  $\mu_1$  of electrons in LT-GaAs layers on the growth temperature.

to an improvement in crystalline quality of layers, and the layer resistance decreases accordingly.

The Ga and As distribution profiles (see examples in Figs. 3, *a* and *b*) suggest that the composition of layers grown at  $T_s < 300^\circ\text{C}$  varied with depth. Regardless of  $T_s$ , near-surface layers (down to a depth of  $\sim 10 \text{ nm}$ ) are enriched with As. Significant fluctuations of Ga and As concentrations are observed near the LT-GaAs/GaAs interface. The As 3d photoelectron line spectra recorded in the examination of LT-GaAs layers grown at temperatures below  $150^\circ\text{C}$  (Fig. 3, *c*) were approximated by three components: the primary one at  $41.5 \text{ eV}$  (As–Ga), the component with a chemical shift of  $+0.9 \text{ eV}$  (associated with elemental As<sup>0</sup> [14]), and the component with a shift of  $-0.5 \text{ eV}$  (As–As dimers [14]). It is likely that arsenic in clusters or interstitial As atoms are detected as elemental As<sup>0</sup>. The net concentration of As<sup>0</sup> and As<sub>dim</sub> at a distance of  $10$ – $20 \text{ nm}$  from the surface of LT-GaAs grown at  $60^\circ\text{C}$  is  $1.5$  at.%. At  $T_s > 150^\circ\text{C}$ , the corresponding concentration is below  $0.5$  at.%, which is comparable to the error of XPS measurements.

A dependence of relative intensity of line As 3d on  $T_s$  (Fig. 3, *d*) was revealed when photoelectron spectra were processed. This is attributable to the spatial anisotropy of photoelectron emission [15]. The shape of dependence of the photoelectron line/background intensity ratio ( $I(\text{As } 3d)/I(15 \text{ eV})$ ) on  $T_s$  implies that the crystalline quality changes slightly at  $T_s = 60$ – $250^\circ\text{C}$ . At  $T_s > 300^\circ\text{C}$ , the layer properties approximate to the characteristics of the substrate.

Thus, pulsed layer deposition is a viable method of synthesis of high-resistance LT-GaAs layers suitable for fabrication of semiconductor devices. The substrate temperature in the process of growth is an important parameter. At  $T_s$  lower than  $300^\circ\text{C}$ , nonuniformities of the chemical composition are observed in layers, and the crystalline quality is rather poor. When the growth temperature exceeds  $300^\circ\text{C}$ , the electron mobility in layers tends to

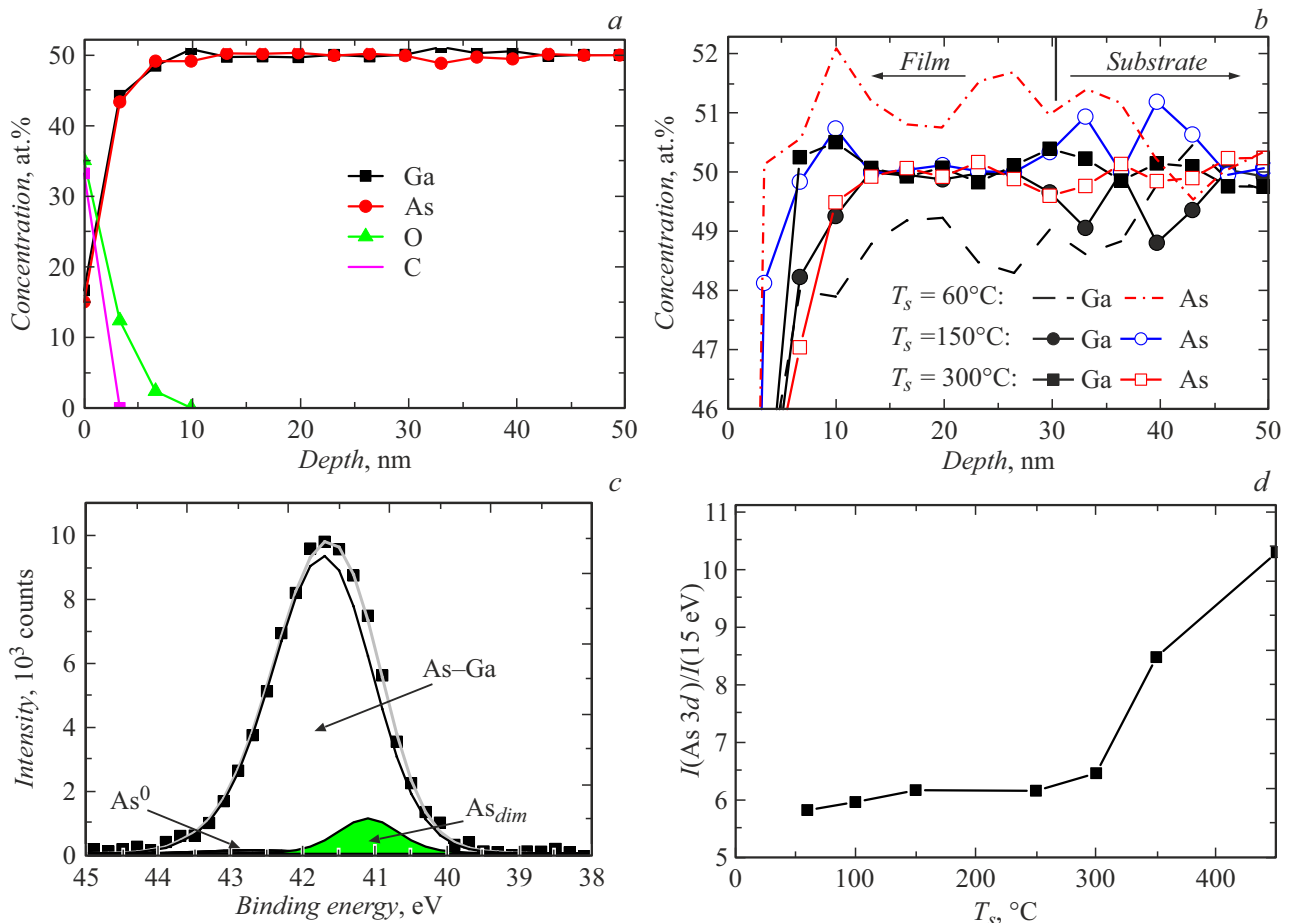


**Figure 3.** *a* — Depth profiles of chemical elements in the LT-GaAs/GaAs structure grown at a temperature of 350°C. *b* — Distribution profiles of Ga and As atoms in LT-GaAs/GaAs structures fabricated at  $T_s = 60, 150$ , and 300°C. *c* — Spectral decomposition of the As 3d photoelectron line recorded in the analysis of the LT-GaAs layer grown at 60°C. The etched layer thickness is 13 nm (points are experimental data, and the gray curve is the sum of spectral components). *d* — Variation of the intensity ratio of the As 3d photoelectron line and the background detected at a binding energy of 15 eV. In signal detection, the analyzer axis was parallel to the normal to the sample surface.

values in excess of  $3000 \text{ cm}^2/(\text{V} \cdot \text{s})$ . This is attributable to an improvement in crystalline quality.

## Funding

This work was supported financially by grant MK-265.2022.1.2 from the President of the Russian Federation. The study of electric properties was performed as part of project No. 23-29-00312 of the Russian Science Foundation.

## Conflict of interest

The authors declare that they have no conflict of interest.

## References

- [1] Y. Horikoshi, M. Kawashima, H. Yamaguchi, Jpn. J. Appl. Phys., **25** (10), L868 (1986). DOI: 10.1143/JJAP.25.L868

- [2] N.A. Bert, A.I. Veinger, M.D. Vilisova, S.I. Goloshechkin, I.V. Ivonin, S.V. Kozyrev, A.E. Kunitsyn, L.G. Lavrent'eva, D.I. Lubyshev, V.V. Preobrazhenskii, B.R. Semyagin, V.V. Tret'yakov, V.V. Chaldyshev, M.P. Yakubanya, Fiz. Tverd. Tela, **35** (10), 2609 (1993) (in Russian).
- [3] A.A. Pastor, P.Yu. Serdobintsev, V.V. Chaldyshev, Semiconductors, **46** (5), 619 (2012). DOI: 10.1134/S106378261205017X.
- [4] A.A. Gorbatshevich, V.I. Egorkin, I.P. Kazakov, O.A. Klimenko, A.Yu. Klokov, Yu.A. Mityagin, V.N. Murzin, S.A. Savinov, V.A. Tsvetkov, Bull. Lebedev Phys. Inst., **42** (5), 121 (2015). DOI: 10.3103/S1068335615050012.
- [5] C. Tannoury, M. Billet, C. Coinon, J.-F. Lampin, E. Peytavit, Electron. Lett., **56** (17), 897 (2020). DOI: 10.1109/IRMMW-THz46771.2020.9370757
- [6] D.S. Abramkin, M.O. Petrushkov, E.A. Emel'yanov, M.A. Putyato, B.R. Semyagin, A.V. Vasev, M.Yu. Esin, I.D. Loshkarev, A.K. Gutakovskii, V.V. Preobrazhenskii, T.S. Shamirzaev, Optoelectron. Instrum. Proc., **54** (2), 181 (2018). DOI: 10.3103/S8756699018020103.

- [7] V.N. Nevedomskii, N.A. Bert, V.V. Chaldyshev, V.V. Preobrazhenskii, M.A. Putyato, B.R. Semyagin, Semiconductors, **43** (12), 1617 (2009).  
DOI: 10.1134/S1063782609120082.
- [8] H. Sakaguchi, T. Mishima, T. Meguro, Y. Fujiwara, J. Phys.: Conf. Ser., **165**, 012024 (2009).  
DOI: 10.1088/1742-6596/165/1/012024
- [9] I. Demir, A.E. Kasapoğlu, H.F. Budak, E. Gür, S. Elagoz, Eur. Phys. J. Appl. Phys., **90** (2), 20301 (2020).  
DOI: 10.1051/epjap/2020190216
- [10] A.V. Kudrin, V.P. Lesnikov, Yu.A. Danilov, M.V. Dorokhin, O.V. Vikhrova, P.B. Demina, D.A. Pavlov, Yu.V. Usov, V.E. Milin, Yu.M. Kuznetsov, R.N. Kriukov, A.A. Konakov, N.Yu. Tabachkova, Semicond. Sci. Technol., **35** (12), 125032 (2020). DOI: 10.1088/1361-6641/abbd5c
- [11] M.P. Seah, W.A. Dench, Surf. Interface Anal., **1** (1), 2 (1979).  
DOI: 10.1002/sia.740010102
- [12] A.V. Boryakov, S.I. Surodin, R.N. Kryukov, D.E. Nikolichev, S.Yu. Zubkov, J. Electron Spectrosc. Relat. Phenom., **229**, 132 (2018). DOI: 10.1016/j.elspec.2017.11.004
- [13] E.V. Kuchis, *Gal'vanomagnitnye effekty i metody ikh issledovaniya* (Radio i Svyaz', M., 1990), pp. 52–55 (in Russian).
- [14] M.V. Lebedev, E. Mankel, T. Mayer, W. Jaegermann, J. Phys. Chem. C, **114** (49), 21385 (2010). DOI: 10.1021/jp104321e
- [15] S. Hofmann, *Auger- and X-ray photoelectron spectroscopy in materials science* (Springer, Berlin, 2013), pp. 30–62.  
DOI: 10.1007/978-3-642-27381-0